Mon. Not. R. Astron. Soc. **000**, 000–000 (0000) Printed 26 January 2007 (MN LATEX style file v2.2)

GRB 060418 and 060607A: the medium surrounding the progenitor and the weak reverse shock emission

Z. P. Jin[1,2] and Y. Z. Fan[1,2,3⋆]
[1] *Purple Mountain Observatory, Chinese Academy of Science, Nanjing 210008, China*
[2] *National Astronomical Observatories, Chinese Academy of Sciences, Beijing 100012, China*
[3] *The Racah Inst. of Physics, Hebrew University, Jerusalem 91904, Israel*

Accepted ..... Received .....; in original form .....

ABSTRACT
We constrain the circum-burst medium profile with the rise behavior of the very early afterglow light curves of gamma-ray bursts (GRBs). Using this method, we find a constant and low-density medium profile for GRB 060418 and GRB 060607A, which is consistent with the inference from the late afterglow data. In addition, we show that the absence of the IR flashes in these two GRB afterglows is consistent with the standard external reverse shock model, which thus renders models like the highly magnetized GRB outflow being unnecessary to a certain extent.

Key words: Gamma Rays: bursts−ISM: jets and outflows–radiation mechanisms: nonthermal

1 INTRODUCTION

Quite recently, Molinari et al. (2007) reported the high-quality very early IR afterglow data of GRB 060418 and GRB 060607A. The IR afterglow lightcurves are characterized by a sharp rise ($\sim t^3$) and then a normal decline ($\sim t^{-1.3}$), though the simultaneous X-ray lightcurves are highly variable. The smooth joint before and after the peak time in the IR band strongly suggests a very weak reverse shock emission.

An interesting usage of these high-quality early afterglow data is to estimate the initial bulk Lorentz factor $\Gamma_{\rm o}$ of the outflow (Molinari et al. 2007). Such an estimate, of course, is dependent of the circumburst medium model (Blandford & McKee 1976; Dai & Lu 1998). For GRB 060418, a wind profile has been ruled out by the late-time X-ray and IR afterglow data (Molinari et al. 2007). While for GRB 060607A, the X-ray data are so peculiar that the medium profile can not be reliably determined. In this work, we use the rise behavior of the very early IR data to pin down the density profile. This new method is valid for both bursts. We show that a constant and low-density medium model is favored. As a result, we confirm that Molinari et al.'s estimation of $\Gamma_{\rm o}$ for GRB 0606418 and GRB 060607A is robust.

The absence of the IR flashes for both bursts are also very interesting. Several possible solutions for non-detection of bright optical flashes in GRB afterglows have been discussed by Roming et al. (2006). To account for this failing detection, it is widely considered that the reverse shock emission would be very weak if the outflow is highly magnetized (Kennel & Coronitti 1984). As shown in the numerical calculation of Fan, Wei & Wang (2004; Fig 1 therein), for the magnetized reverse shock, its peak optical/IR emission increases with σ for $\sigma \leq 0.1$, then decreases for larger σ, where σ refers to the ratio of the magnetic energy density to the particle energy density of the GRB outflow. Quite similar results have also been obtained in the analytical investigation of Zhang & Kobayashi (2005). In principle, the non-detection of the optical flashes could be interpreted if $\sigma \gg 1$. This conclusion motivated Molinari et al. (2007) to suggest these two GRB outflows might be magnetized. However, in this work we show that for these two bursts, the absence of the IR flashes are actually consistent with the standard external reverse shock model (Sari & Piran 1999a; Mészáros & Rees 1999; Kobayashi 2000) and thus render the magnetized outflow model unnecessary or alternative.

2 VERY EARLY AFTERGLOW: CONSTRAINT ON THE MEDIUM PROFILE

In this section we discuss the forward shock emission because the data show no evidence for a dominant reverse shock component.

Firstly, we discuss a constant and low-density medium model. For $t < t_\times$, the fireball has not been decelerated significantly by the medium, where $t_\times$ is the time when the reverse shock crosses the outflow. The bulk Lorentz factor

⋆ Golda Meir Fellow, E-mail: yzfan@pmo.ac.cn

Γ is thus nearly a constant, so is the typical synchrotron frequency ν_m (Sari et al. 1998). On the other hand, the maximal specific flux $F_{\nu,\max} \propto N_{\rm e} \propto t^3$, where $N_{\rm e}$ is the total number of the electrons swept by the forward shock. We thus have

$$F_{\rm obs} \propto F_{\nu,\max}(\nu_{\rm obs}/\nu_m)^{-(p-1)/2} \propto t^3, \quad (1)$$

for $\nu_m < \nu_{\rm obs} < \nu_c$, where ν_c is the cooling frequency and $\nu_{\rm obs}$ is the observer's frequency. This temporal behavior is perfectly consistent with the current data.

Secondly, we discuss a wind medium with a density profile $n_{\rm w} = 3.0 \times 10^{35}$ cm^{-3} $A_* R^{-2}$, where R is the radius of the shock front to the central engine, $A_* = [\dot{M}/10^{-5} M_\odot$ yr$^{-1}][v_w/(10^8 {\rm cm\ s^{-1}})]$, $\dot{M}$ is the mass loss rate of the progenitor, v_w is the velocity of the stellar wind. Again, for $t < t_\times$, the bulk Lorentz factor of the fireball Γ is nearly a constant (Chevalier & Li 2000). However, in this case, $\nu_m^w \propto t^{-1}$, $\nu_c^w \propto t$ and $F_{\nu,\max}^w \propto t^0$, where the superscript "w" represents the parameter in the wind case. The increase of the forward shock emission can not be steeper than $t^{1/2}$, as long as the self-absorption effect can be ignored (Chevalier & Li 2000). This temporal behavior, of course, is inconsistent with the data. Can the synchrotron self-absorption shape the forward shock emission significantly and then render the wind model likely? Let's examine this possibility. In this interpretation, $\nu_a^w(t_{\rm IR,peak}) \sim 2 \times 10^{14}$ Hz is required, where ν_a is the synchrotron self-absorption frequency of the forward shock electrons, and $t_{\rm IR,peak}$ is the peak time of the IR-band emission. In the wind model, to get a $t^{-1.3}$ IR-band light curve, we need $p \sim 2$ and $\nu_m^w < \nu_a^w < \nu_{\rm obs} < \nu_c^w$. Following Chevalier & Li (2000), it is straightforward to show that $\nu_a^w \sim 5 \times 10^{13}$ Hz $\epsilon_{e,-1}^{1/3} \epsilon_{\rm B,-2}^{1/3} A_*^{2/3} t_{d,-3}^{-1}$ and $\nu_c^w \sim 3.5 \times 10^{13}$ Hz $\epsilon_{B,-2}^{-3/2} E_{\rm k,54}^{1/2} A_*^{-2} [(1+z)/2]^{-3/2} t_{d,-3}^{1/2} (1+Y^w)^{-2}$, where ϵ_e and ϵ_B are the fractions of shock energy given to the electrons and magnetic field, respectively; z is the redshift, t_d is the observer's time in units of day, and $E_{\rm k}$ is the isotropic-equivalent kinetic energy of the outflow. Here and throughout this text, the convention $Q_x = Q/10^x$ has been adopted in cgs units.

With the requirements that at $t_{\rm IR,peak} \sim 150$s, $\nu_a^w \sim 2 \times 10^{14}$ Hz and $\nu_c^w > 2 \times 10^{14}$ Hz, we have

$$\epsilon_{e,-1}^{1/3} \epsilon_{\rm B,-2}^{1/3} A_*^{2/3} \sim 8, \quad (2)$$

$$\epsilon_{B,-2}^{-3/2} E_{\rm k,54}^{1/2} A_*^{-2} > 4(1+Y^w)^2. \quad (3)$$

These two relations yield $\epsilon_B < 2 \times 10^{-5} (1+Y^w)^{-4} E_{k,54} \epsilon_e^2$ and $A_* > 160\ \epsilon_e^{-3/2} E_{k,54}^{-1/2} (1+Y^w)^2$. For such a large contrast between ϵ_e and ϵ_B, $Y^w \gg 1$. The resulting ϵ_B and A_* are too peculiar to be acceptable.

Therefore it is very likely that the medium surrounding the GRB progenitor has a low and constant number density. This conclusion is also supported by the temporal and spectral analysis of the late time X-ray and IR afterglows of GRB 060418 (Molinari et al. 2007). Here it is worth pointing out that though the multi-wavelength afterglow modeling of many other bursts has reached a similar conclusion (Panaitescu & Kumar 2001), these works were only based on the late-time afterglow data and may be invalid for the early ones. This is because the density profile of the circumburst medium, in principle, could vary over radius due to the interaction between the stellar-wind and the interstellar medium. For $R < R_c \sim$ several $\times 10^{16} - 10^{17}$cm, the medium may be wind-like. At larger R, the stalled wind material may be ISM-like (Ramirez-Ruiz et al. 2001). Assuming that GRB 060418 has such a density profile, we can estimate R_c as follows. Note that at R_c, the outflow has not got decelerated, which implies that $3.8 \times 10^{36} A_* \Gamma^2 m_p c^2 < E_k/2$. On the other hand, at $t_{\rm IR,peak}$ a $\Gamma_\times \sim 200$ is likely (Molinari et al. 2007). We thus have

$$R_c < 2 \times 10^{15}\ {\rm cm}\ E_{k,54} A_*^{-1}. \quad (4)$$

3 INTERPRETING THE ABSENCE OF THE REVERSE SHOCK EMISSION

3.1 General relation between forward and reverse shock peak emission: the thin fireball case

In the standard fireball afterglow model, there are two shocks formed when the fireball interacts with the medium (Piran 1999), one is the ultra-relativistic forward shock emission expanding into the medium, the other is the reverse shock penetrating into the GRB outflow material. The forward shock is long-lasting while the reverse shock is short-living. At a time $t_\times \sim \max\{T_{90}, 60(1+z) E_{k,54}^{1/3} n_0^{-1/3} \Gamma_{\rm o,2.5}^{-8/3}\}$, the reverse shock crosses the GRB outflow, where n is the number density of the medium (please note that a dense wind medium has been ruled out for these two bursts) and $\Gamma_{\rm o}$ is the initial Lorentz factor of the GRB outflow.

If the fireball is thick, $t_\times \sim T_{90}$. The reverse shock emission overlaps the prompt $\gamma-$rays and is not easy to be detected (Sari & Piran 1999b; Kobayashi 2000). In this work, we focus on the *thin fireball case*, in which the peak of the reverse shock emission and the prompt $\gamma-$rays are separated. The relatively longer reverse shock emission renders it more easily to be recorded by the observers. In this case,

$$t_\times \sim 60(1+z)\ {\rm s}\ E_{k,54}^{1/3} n_0^{-1/3} \Gamma_{\rm o,2.5}^{-8/3}. \quad (5)$$

After that time, the dynamics of the forward shock can be well approximated by the Blandford-McKee similar solution (Blandford & McKee 1976), which emission can be estimated by

$$F_{\nu,\max} = 6.6\ {\rm mJy}\ (\frac{1+z}{2}) D_{L,28.34}^{-2} \epsilon_{B,-2}^{1/2} E_{k,53} n_0^{1/2}, \quad (6)$$

$$\nu_m = 2.4 \times 10^{16}\ {\rm Hz}\ E_{\rm k,53}^{1/2} \epsilon_{\rm B,-2}^{1/2} \epsilon_{e,-1}^2 C_p^2 (\frac{1+z}{2})^{1/2} t_{d,-3}^{-3/2}, \quad (7)$$

$$\nu_c = 4.4 \times 10^{16}\ {\rm Hz}\ E_{k,53}^{-1/2} \epsilon_{B,-2}^{-3/2} n_0^{-1} (\frac{1+z}{2})^{-1/2} t_{d,-3}^{-1/2} \frac{1}{(1+Y)^2}, \quad (8)$$

where p is the power-law index of the shocked electrons, $C_p \equiv 13(p-2)/[3(p-1)]$, the Compton parameter $Y \sim (-1+\sqrt{1+4\eta\epsilon_e/\epsilon_B})/2$, $\eta \sim \min\{1, (\nu_m/\bar{\nu}_c)^{(p-2)/2}\}$ and $\bar{\nu}_c = (1+Y)^2 \nu_c$.

Following Zhang et al. (2003) and Fan & Wei (2005), we assume that $\epsilon_e^{\rm r} = \mathcal{R}_{\rm e} \epsilon_{\rm e}$ and $\epsilon_{\rm B}^{\rm r} = \mathcal{R}_{\rm B}^2 \epsilon_{\rm B}$, where the superscript "r" represents the parameter of the reverse shock. At $t_\times$, the reverse shock emission are governed by (Fan & Wei 2005)

$$\nu_{\rm m}^{\rm r}(t_\times) = \mathcal{R}_{\rm B}[\mathcal{R}_{\rm e}(\gamma_{34,\times} - 1)]^2 \nu_{\rm m}(t_\times)/(\Gamma_\times - 1)^2, \quad (9)$$

$$\nu_{\rm c}^{\rm r}(t_\times) \approx \mathcal{R}_{\rm B}^{-3}[(1+Y)/(1+Y^{\rm r})]^2 \nu_{\rm c}, \quad (10)$$

$$F_{\nu,\max}^{\rm r}(t_\times) \approx \Gamma_{\rm o} \mathcal{R}_{\rm B} F_{\nu,\max}(t_\times), \quad (11)$$

where $\gamma_{34,\times} \approx (\Gamma_{\rm o}/\Gamma_\times + \Gamma_\times/\Gamma_{\rm o})/2$ is the Lorentz factor

of the shocked ejecta relative to the initial outflow (note that we focus on the "thin fireball case"), $\Gamma_\times \sim \Gamma_{\rm o}/2$ is the bulk Lorentz factor of the shocked ejecta at $t_\times$, $Y^{\rm r} \simeq [-1+\sqrt{1+4\eta^{\rm r}\mathcal{R}_{\rm e}\epsilon_{\rm e}/(\mathcal{R}_{\rm B}^2\epsilon_{\rm B})}]/2$ is the Compton parameter, $\eta^{\rm r} \approx \min\{1,\ (\nu_{\rm m}^{\rm r}/\bar{\nu}_{\rm c}^{\rm r})^{({\rm p}-2)/2}\}$ and $\bar{\nu}_c^{\rm r} = (1+Y^{\rm r})^2\nu_c^{\rm r}$.

With the observer frequency $\nu_{\rm obs}$, $\nu_m^{\rm r}(t_\times)$, $\nu_c^{\rm r}(t_\times)$ and $F_{\nu,\max}^{\rm r}(t_\times)$, it is straightforward to estimate the peak flux of the reverse shock emission (Sari & Piran 1999a). For the IR/optical emission (i.e., $\nu_{\rm obs} \sim 2-5\times10^{14}$ Hz) that interests us here, we usually have $\nu_m^{\rm r} < \nu_{\rm obs} < \nu_c^{\rm r}$. The observed reverse shock emission is thus

$$F_{\rm obs}^{\rm r}(t_\times) \approx F_{\nu,\max}^{\rm r}(t_\times)[\nu_{\rm obs}/\nu_m^{\rm r}(t_\times)]^{-(p-1)/2}. \quad (12)$$

With eq.(6) and the relation $\Gamma_\times \sim \Gamma_{\rm o}/2$, we have

$$\begin{aligned}\frac{F_{\rm obs}^{\rm r}(t_\times)}{F_{\nu,\max}} &\approx \Gamma_{\rm o}\mathcal{R}_{\rm B}^{\frac{(p+1)}{2}}[\frac{\mathcal{R}_{\rm e}(\gamma_{34}(t_\times)-1)}{\Gamma(t_\times)-1}]^{p-1}[\frac{\nu_{\rm obs}}{\nu_m(t_\times)}]^{\frac{-(p-1)}{2}} \\ &\approx 2^{1-{\rm p}}\Gamma_{\rm o}^{2-{\rm p}}\mathcal{R}_{\rm e}^{{\rm p}-1}\mathcal{R}_{\rm B}^{\frac{{\rm p}+1}{2}}[\frac{\nu_{\rm obs}}{\nu_m(t_\times)}]^{\frac{-(p-1)}{2}} \\ &\approx 0.08\mathcal{R}_{\rm e}^{{\rm p}-1}\mathcal{R}_{\rm B}^{\frac{{\rm p}+1}{2}}[\frac{\nu_{\rm obs}}{\nu_m(t_\times)}]^{\frac{-(p-1)}{2}}, \quad (13)\end{aligned}$$

where $p \sim 2.3$ and $\Gamma_{\rm o} \sim 200$ have been taken into account. Eq.(13) is the main result of this paper. *It is now evident that to have a* $F_{\rm obs}^{\rm r}(t_\times) \geq F_{\nu,\max}$*, we need* $\mathcal{R}_{\rm e} \gg 1$*, or* $\mathcal{R}_{\rm B} \gg 1$*, or* $\nu_{\rm obs} \ll \nu_m(t_\times)$*, or both.* If $\nu_{\rm obs} \ll \nu_m(t_\times) < \nu_c(t_\times)$, the forward shock will peak at a time t_p when $\nu_m(t_p) \approx (t_p/t_\times)^{-3/2}\nu_m(t_\times) \approx \nu_{\rm obs}$. So eq.(13) can be re-written as

$$\frac{F_{\rm obs}^{\rm r}(t_\times)}{F_{\nu,\max}} \approx 0.08\mathcal{R}_{\rm e}^{{\rm p}-1}\mathcal{R}_{\rm B}^{\frac{{\rm p}+1}{2}}(\frac{t_p}{t_\times})^{\frac{3(p-1)}{4}}. \quad (14)$$

In the standard reverse shock model (Sari & Piran 1999a; Mészáros & Rees 1999; Kobayashi 2000), $\mathcal{R}_{\rm e} = \mathcal{R}_{\rm B} = 1$. So to have a bright optical flash to outshine the forward shock emission, we need

$$\nu_m(t_\times) > 125^{1/({\rm p}-1)}\nu_{\rm obs} \ \text{ or } \ t_p > 29^{1/(p-1)}t_\times. \quad (15)$$

For typical GRB forward shock parameters $\epsilon_{e,-1} \sim \epsilon_{B,-2} \sim E_{\rm k,53} \sim 1$ and $p \sim 2.3$, at $t_\times \sim 100$ s, we have $\nu_m(t_\times) \sim 50\nu_{\rm obs}$ and $F_{\rm obs}^{\rm r}(t_\times) \sim F_{\nu,\max}$. This simple estimate is consistent with the results of some recent/detailed numerical calculations (Nakar & Piran 2004; McMahon et al. 2006; Yan et al. 2007).

However, it is not clear whether these parameters, derived from modelling the late afterglow data (Panaitescu & Kumar 2001), are still valid for the very early afterglow data. We need high-quality early IR/optical afterglow data to pin down this issue.

3.2 Case study

Analytical approach. For GRB 060418 and GRB 060607A, their parameters (T_{90}, z, $E_{\gamma,52}$, $F_{\rm IR,peak}$, $t_{\rm IR,peak}$) are (50s, 1.489, 9, 50mJy, 153s) and (100s, 3.082, 10, 20mJy, 180s), respectively (Molinari et al. 2007). Here E_γ is the isotropic-equivalent prompt gamma-ray energy. As shown in Molinari et al. (2007), for $t > t_{\rm IR,peak}$, both the temporal and the spectral data of GRB 060418 are well consistent with a slow-cooling fireball expanding into a constant medium. To interpret the afterglow of GRB 060607A, however, is far more challenging. We note that the ratio between the X-ray flux and the IR flux increases with time sharply and the late time X-ray afterglow flux drops with time steeper than[1] t^{-4}. These two peculiar features, of course, can not be interpreted normally. One speculation is that nearly all the X-ray data are the so-called "central engine afterglow" (i.e., the afterglow attributed to the prolonged activity of the central engine) and are independent of the IR afterglow (Fan & Wei 2005). This kind of ad hoc speculation is hard to be confirmed or to be ruled out. However, the similarity between these two early IR band afterglow light curves implies that both of them may be the forward shock emission of a slow-cooling fireball.

Hereafter we focus on GRB 060418. The peak H-band flux is ~ 50 mJy, while the peak X-ray emission attributed to the forward shock emission is likely to be ~ 0.15 mJy (Molinari et al. 2007). The contrast is just ~ 300, which suggests a $\nu_{\rm c}(t_{\rm IR,peak}) \sim 2.4\times10^{17}$ Hz, where a $p = 2.6\pm0.1$ has been taken into account (Molinari et al. 2007). On the other hand, in the slow cooling phase, the observed flux peaks because the observer's frequency crosses ν_m or the peak time $\sim t_\times$ for $\nu_m < \nu_{\rm obs}$. So we have two more constraints: $\nu_m(t_{\rm IR,peak}) \leq 1.8\times10^{14}$ Hz and $F_{\nu,\max} \geq 50$ mJy.

With eqs.(6-8), it is straightforward to show that

$$\epsilon_{B,-2}^{1/2}E_{\rm k,53}n_0^{1/2} \geq 20, \quad (16)$$

$$\epsilon_{B,-2}^{1/2}E_{\rm k,53}^{1/2}\epsilon_{e,-1}^2 \leq 6\times10^{-3}, \quad (17)$$

$$\epsilon_{B,-2}^{-3/2}E_{\rm k,53}^{-1/2}n_0^{-1}(1+Y)^{-2} \sim 8. \quad (18)$$

These relations are satisfied with ($E_{\rm k,53}$, n_0, ϵ_e, ϵ_B, p) $\sim$ (100, 1, 0.004, 0.001, 2.6).

Is $t_\times \sim t_{\rm IR,peak}$? The answer is positive. If $t_\times < t_{\rm IR,peak}$, the IR band flux will increase with time as t^3 for $t \leq t_\times$ and then change with time as $t^{1/2}$ for $t_\times < t < t_{\rm IR,peak}$ (Sari et al. 1998). This is inconsistent with the observation. So we have $t_\times \sim t_{\rm IR,peak} > T_{90}$ and the fireball is thin. Our assumption made in the last subsection is thus valid. Now $\nu_{\rm m}(t_\times) \approx \nu_{\rm m}(t_{\rm IR,peak}) \leq \nu_{\rm obs}$. With eq.(13) and $\mathcal{R}_{\rm e} = \mathcal{R}_{\rm B} = 1$, we have

$$\frac{F_{\rm obs}^{\rm r}(t_\times)}{F_{\nu,\max}} \sim \mathcal{O}(0.1). \quad (19)$$

So the reverse shock emission is too weak to dominate over that of the forward shock. The non-detection of the IR flashes in GRB 060418 and GRB 060607A has then been well interpreted.

Numerical fit to the afterglow of GRB 060418. The code used here to fit the multi-band lightcurves has been developed by Yan et al. (2007), in which both the reverse and the forward shock emission have been taken into account. As mentioned in the analytical investigation, the X-ray data are flare-rich. These flares, of course, are very hard to be understood in the external forward shock model. Instead it may be attributed to the prolonged activity of the central engine. Assuming that the power-law decaying part (i.e., excluding the flares) is the forward shock emission, the small

[1] In the jet model, the flux declines with time as $\max\{t^{-p},\ t^{-(2+\beta)}\}$ for $p < 4$ when we have seen the whole ejecta, where $\beta \leq p/2$ is the spectral index of the collected photons. So we need a quite unusual $p \geq 5$ to account for such a steep X-ray decline.

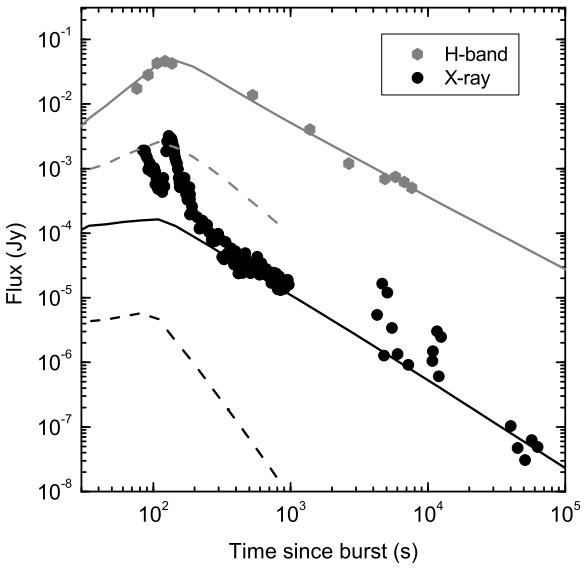

Figure 1. Numerical fit to the afterglow of GRB060418. The solid and dashed lines represent the emission from the forward and reverse shock.

contrast between the X-ray and the H-band flux at $t_{\rm IR,peak}$ requires a $\nu_{\rm c} \sim 2.4 \times 10^{17}$ Hz and thus a small $\epsilon_{\rm B}$ and a normal n. The very early peak of the IR-band afterglow light curves strongly suggests an unusual small ϵ_e. The relatively bright IR-band peak emission implies a very large $E_{\rm k}$.

Our numerical results have been presented in Fig.1. The best fit parameters are $(E_{\rm k,53},\ n_0,\ \epsilon_e,\ \epsilon_B,\ p,\ \Gamma_0) \sim$ (300, 1, 0.005, 0.0002, 2.5, 600). The reverse shock emission is too weak to outshine the forward shock emission (note that in this work, $\mathcal{R}_{\rm e} = \mathcal{R}_{\rm B} = 1$ are assumed), as predicted before. In the calculation, we did not take into account the external Inverse Compton (EIC) cooling by the flare photons. Here we discuss it analytically. Following Fan & Piran (2006), the EIC cooling parameter can be estimated by $Y_{\rm EIC} \sim 0.4 L_{\rm flare,48.7} \epsilon_{\rm B,-3.7}^{-1} E_{\rm k,55.5}^{-1} \Delta T_3$, where $L_{\rm flare}$ is the luminosity of the flare and ΔT is the duration of the flare. Such a cooling correction is so small that can be ignored.

The half-opening angle θ_j of the ejecta can not be well determined with the current data. The lack of the jet break in H-band up to $t_d \sim 0.1$ suggests a $\theta_j > 0.024$. So a robust estimate of the intrinsic kinetic energy of GRB 060418 is $\sim E_{\rm k}\theta_j^2/2 > 8 \times 10^{51}$ erg.

4 SUMMARY

The temporal behavior of the very early afterglow data is valuable to constrain the medium profile surrounding the progenitor. For GRB 060418 and GRB 060607A, the sharp increase of the very early H-band afterglow light curve has ruled out a WIND-like medium. This conclusion is further supported by the late time X-ray and IR afterglow data of GRB 060418. This rather robust argument is inconsistent with the canonical collapsar model, in which a dense stellar wind medium is expected. More fruitful very early IR/optical data are needed to draw a more general conclusion.

The absence of the reverse shock signatures in the high-quality IR afterglows of GRB 060418 and GRB 060607A may indicate the outflows being strongly magnetized. We, instead, show that the non-detection of IR flashes in these two events is consistent with the standard reverse shock model and thus render the magnetization scenario unnecessary or alternative. The physical reason is that in these two bursts, $\nu_m(t_\times) \sim 2 - 5 \times 10^{14}$ Hz. Such a small $\nu_m(t_\times)$ will influence our observation in two respects. One is that $\nu_m^{\rm r}(t_\times) \sim \nu_m(t_\times)/4\Gamma_{\rm o}^2 \sim 10^9$Hz. The corresponding emission in IR band is thus very weak. The other is that now the forward shock peaks at IR/optical band at $t_\times$. Consequently, the IR/optical emission of the reverse shock can not dominate over that of the forward shock.

It is not clear whether the absence of the optical flashes in most GRB afterglows (Roming et al. 2006) can be interpreted in this way or not. Of course, one can always assume $\mathcal{R}_{\rm e} \ll 1$ or/and $\mathcal{R}_{\rm B} \ll 1$ to solve this puzzle. But before adopting these phenomenological approaches, one may explore the physical processes that could give rise to these modifications. Anyway, we do have found in some bursts, for example, GRB 050319 (Mason et al. 2006), GRB 050401 (Rykoff et al. 2005), and GRB 061007 (Schady et al. 2007), the optical afterglow flux drops with time as a single power for $t >$ several $\times$ 100 s and strongly implies a very small $\nu_m(t_\times)$. It is likely that the non-detection of the IR/optical flash in some bursts are consistent with the standard reverse shock model and thus not to our surprise.

ACKNOWLEDGMENTS

We thank Bing Zhang and Daming Wei for discussion, and Daniele Malesani and Ting Yan for kind help. This work is supported by the National Natural Science Foundation (grant 10673034) of China.

REFERENCES

Blandford R. D., McKee C. F., 1976, Phys. Fluids., 19, 1130
Chevalier R. A., Li Z. Y., 2000, ApJ, 536, 195
Dai Z. G., Lu T., 1998, MNRAS, 298, 87
Fan Y. Z., Piran T., 2006, MNRAS, 370, L24
Fan Y. Z., Wei D. M., 2005, MNRAS, 364, L42
Fan Y. Z., Wei D. M., Wang C. F., 2004, A&A, 424, 477
Kennel C. F., & Coronitti E. V., 1984, ApJ, 283, 694
Kobayashi S., 2000, ApJ, 545, 807
McMahon E., Kumar P., Piran, T., 2006, MNRAS, 366, 575
Mason K. O., et al., 2006, ApJ, 639, 361
Mészáros, P., & Rees, M. J., 1999, MNRAS, 306, L39
Molinari E. et al. , 2007 (astro-ph/0612607)
Nakar E., Piran T., 2004, MNRAS, 353, 647
Panaitescu A., Kumar P., 2001, ApJ, 560, 49
Piran T., 1999, Phys. Rep., 314, 575
Ramirez-Ruiz E, Dray L. M., Madau P., Tout C. A., 2001, MNRAS, 327, 829
Roming, P. W. A., et al. , 2006 , ApJ, 652, 1416
Rykoff E. S., et al. 2005, ApJ, 631, L121
Sari R., Piran T., 1999a, ApJ, 517, L109

Sari R., Piran T., 1999b, ApJ, 520, 641
Sari R., Piran T., Narayan R., 1998, ApJ, 497, L17
Schady P., 2007, MNRAS, submittd (astro-ph/0611081)
Yan T., Wei D. M., Fan Y. Z., 2007 (astro-ph/0512179)
Zhang B., Kobayashi S., 2005, ApJ, 628, 315
Zhang B., Kobayashi S., Mészáros P., 2003, ApJ, 595, 950